Accelerated high-resolution imaging of trabecular bone using total variation constrained reconstruction

M. J. Wald[1], G. Adluru[1], H. K. Song[1], and F. W. Wehrli[1]

[1]Laboratory for Structural NMR Imaging, University of Pennsylvania Medical Center, Philadelphia, Pennsylvania, United States

Introduction: High-resolution micro-magnetic imaging (μMRI) of trabecular bone (TB) allows the assessment of topological changes associated with bone disease[1] and treatment efficacy[2]. Digital topological analysis (DTA)[3] involves classifying bone voxels as belonging to different topological entities, such as a surface, curve or junction between these voxel types. Classification is sensitive to SNR, which is limited by the high-resolutions necessary to resolve trabeculae (~100-200μm). Parallel imaging techniques permit shortening scan times by utilizing RF coil encoding from multiple receiver coils. However, high acceleration factors are mired by the associated loss in SNR and noise amplification caused by coil geometry. It has recently been shown that constrained reconstruction/compressed sensing techniques[4,5] can be used to accelerate MRI acquisitions. These methods exploit implicit sparsity in the data and do not contribute to noise amplification, and therefore may be advantageous in situations demanding higher acceleration factors (R), particularly when limited by the number of RF coil channels and/or the object's geometry. Here we explore the application of Total Variation Constrained Reconstruction (TVCR) to TB imaging and compare the method in terms of the derived topological parameters with generalized partially-parallel acquisition (GRAPPA).

Theory: Unlike GRAPPA reconstruction in which an alias-free image is obtained by utilizing coil sensitivity encoding[6], in TVCR, an alias-free image m^* from fractional k-space data d' is obtained by iteratively minimizing a cost function according to Equation 1 which consists of a data fidelity term (first term) and a spatial total variation[7] constraint term (second term). The data fidelity term ensures that the final reconstructed image m' is consistent with the acquired data d'. The encoding operator E computes the Fourier transform of the image at the k-space grid-points of the acquired data d'. The constraint term represents the L1 norm of the spatial gradient ∇_{xy} of the image, which penalizes the intensity variations in the image due to undersampling. The regularization parameter α controls the tradeoff between the two terms.

$$m^* = \arg\min\left[\left\|Em'-d\right\|_2^2 + \alpha\left\|\nabla_{xy} m'\right\|_1^1\right] \qquad (1)$$

Methods: A demarrowed human distal tibia specimen, fixed in 100mMol Gd-DTPA 10% formalin solution (T_1 =300ms), was imaged using a modified FLASE pulse sequence[8] with a voxel size of $(160\mu m)^3$ over a field-of-view of $80x64x10mm^3$ in 26mins(64 slices). Data was acquired on a Siemens TIM Trio 3T scanner (Erlanger, Germany) using a four-channel RF coil (Insight MRI, Worcester, MA). The fully sampled k-space was decimated in a variable density pattern to retain 220, 160, 130, and 112 phase encoding (PE_y) lines (out of 400 total) to simulate R=1.8, 2.5, 3.1, and 3.6 accelerated acquisitions, respectively. Forty central PE_y lines were retained for each R value. The remaining PE_y lines were pseudo-randomly distributed in the high-spatial frequency region for TVCR while they were uniformly spaced for GRAPPA. TVCR was performed by iteratively minimizing the cost function in Eq.1 using gradient descent technique[9] while the GRAPPA reconstructions were done with an auto-calibrated 5x6 (columns x lines) interpolation matrix. Each sum-of-squares reconstruction was masked, bone-volume-fraction-mapped[10], skeletonized[11], and DTA-processed[3]. The % error of the bone volume fraction (BV/TV) and surface-to-curve ratio (S/C=surface voxel density/curve voxel density) were calculated for each R relative to the full acquisition.

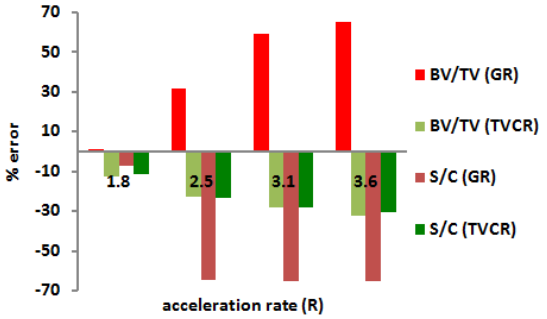

Fig. 1. Sensitivity (% error relative to 26 minute acquisition) of apparent BV/TV and S/C relative to R for GRAPPA(GR) and TVCR. R=3.6 corresponds to a ~7 minute scan.

Results and Discussions: In Fig. 1, the sensitivities (% error) of the apparent BV/TV and S/C relative to R are plotted for both reconstructions. While more precise for R=1.8, BV/TV and S/C derived from the GRAPPA images are considerably more sensitive to increases in R than the TVCR approach. Image slices from the full acquisition and the GRAPPA and TVCR for R=1.8 and R=3.1 are shown in Fig. 2a-e. Although SNR is not easily comparable between the two reconstructions, noise inflation is apparent in the GRAPPA reconstructions (Fig. 2b&d). The loss of SNR, as seen in Fig. 2d, is attributed to poor encoding performance for R>2 using a curved four channel RF coil, resulting in very large errors (59% and 65% for BV/TV and S/C respectively) at R=3.1. Some degree of blurring and thinning of the TB structure is evident in the R=3.1 TVCR image (Fig. 1e). Apparent BV/TV and S/C computed in the TVCR images decrease with increasing R (-26% for both at R=3.1). S/C decreases due to loss of surface voxel density (-25% at R=3.1) while curve voxel density marginally increased (+4% at R=3.1) at higher R. This effect is likely the result of the thinning of the structure as seen in Figs. 1c&e.

Conclusions: The topological parameters derived from the GRAPPA reconstructions at high acceleration factors (R>2) are affected by loss in SNR to a greater extent than those derived from TVCR images. Initial results show promise for TVCR as a means to reduce scan time in μMRI of TB beyond that achievable with partial-parallel imaging without a dramatic loss in sensitivity to the TB microstructure.

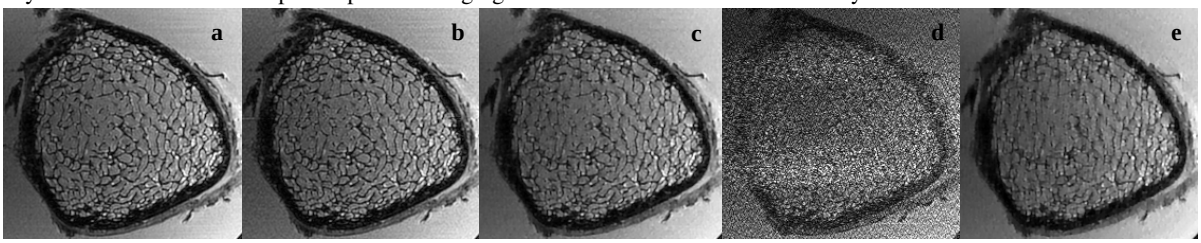

Fig. 2. Images from distal tibia specimen. a) Fully sampled (26 mins) FLASE acquisition; b) GRAPPA R=1.8; c) TVCR R=1.8; d) GRAPPA R=3.1; e) TVCR R=3.1.

References: **[1]** F.W.Wehrli et al., *JBMR* 23, 730 (2008). **[2]** M.Benito et al., *JBMR* 20, 1785 (2005). **[3]** B.R.Gomberg et al., *IEEE TMI* 19, 166 (2000). **[4]** K.T. Block et al., *MRM* 57, 1086 (2007). **[5]** M.Lustig et al., *MRM* 58, 1182 (2007). **[6]** M.A.Griswold et al., *MRM* 47, 1202 (Jun, 2002). **[7]** L.Rudin et al., *Physica D* 60, 259 (1992). **[8]** J.Ma et al., *MRM* 35, 903 (1996). **[9]** G.Adluru et al., *ISBI*, Washington, DC (2007). **[10]** B.Vasilic,F. W.Wehrli,*IEEE TMI* 24, 1574 (2005). [**11**] J.M. Magland, F. W. Wehrli, *Acad. Radio.* In press (2008). **Acknowledgements:** NIH F31EB74482, RO1 AR41443, RO1 AR53156, ACSRSG-08-118-01-CCE